

# N\* Experiments and their Impact on Strong QCD Physics

Volker D. Burkert  
for the CLAS collaboration

March 28, 2018

**Abstract** I give a brief report on experimental studies of the spectrum and the structure of the excited states of the nucleon and what we learn about their internal structure. The focus is on the effort to obtain a more complete picture of the light-quark baryon excitation spectrum employing electromagnetic beams, and on the study of the transition form factors and helicity amplitudes and their dependence on the size of the four-momentum transfer  $Q^2$ , especially on some of the most prominent resonances. These were obtained in pion and eta electroproduction experiments off proton targets.

**Keywords** light-quark excitation, baryon spectrum, electroexcitation of nucleon resonances, quark core, meson-baryon contributions

**PACS** 12.39.Ki, 13.30.Eg, 13.40.Gp, 14.20.Gk

## 1 Introduction

For this introductory talk the organizers asked to address what we learn about strong QCD (sQCD) from the study of nucleon resonances transitions. Nathan Isgur said in the concluding talk at N\*2000: "*I am convinced that completing this chapter in the history of science will be one of the most interesting and fruitful areas of physics for at least the next thirty years.*"

We begin this conference in excited anticipation of tomorrow's solar eclipse, which, thanks to the organizers schedule, coincides with the second day of this conference. It allows me to refer to another famous Solar Eclipse of March 29, 1919, when Sir Arthur Eddington performed the first experimental test [1] of Albert Einstein's general theory of relativity [2]. The findings led to the

---

Volker D. Burkert  
Thomas Jefferson National Accelerator Facility  
Newport News, Virginia 23606, USA  
E-mail: burkert@jlab.org

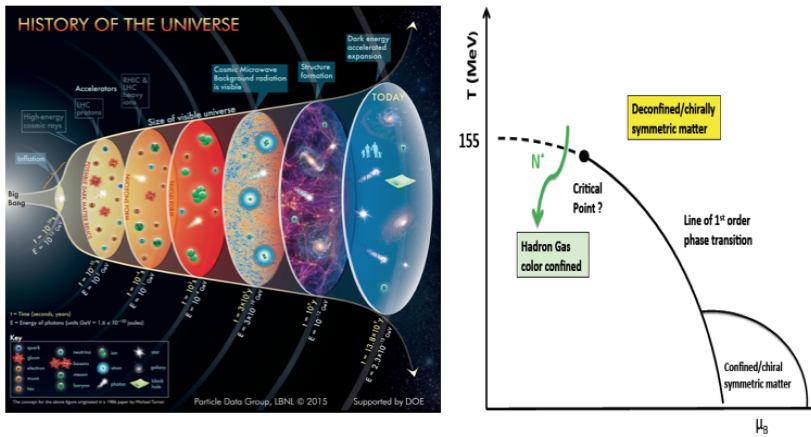


**Fig. 1** Left panel: The evolution of the Universe as depicted by the LBNL Particle Data Group, 2015. The area characterized by the second disk from the left is where hadrons of confined quarks and gluons occur. The CEBAF electron accelerator has the energy reach to access this region and study processes in isolation that occurred in the microsecond old universe and resulted in the freeze out of baryons. Right panel: A generic phase diagram for the transition from the de-confined quark-gluon state to the confined hadron state.

eventual triumph of general relativity over classical Newtonian physics. It also gave birth to modern scientific cosmology and the study of the history of the universe.

In this meeting we also address how excited states of the nucleon fit into our understanding of the forces and the dynamics of matter in the history of the universe and in its current state. The Particle Data Group issues the beautiful representations of the phases through which the universe evolved from the Big Bang (BB) to our times as shown in Fig. 1. There are some marked events that have been of particular significance during the early phases of its history, such as the quark-gluon plasma (QGP) of non-interacting color quarks and gluons, the forming of nucleons, and of light nuclei. What is not shown, but is of particular significance for our field, is the transition from the QGP to stable nucleons that begins just microseconds after the BB, when dramatic events occurred - chiral symmetry is broken, quarks acquire mass dynamically, baryon resonances occur abundantly, and quarks and gluons become confined in nucleons. This crossover process is controlled by the excited hadrons, as is schematically shown in the generic QCD phase diagram in Fig. 1. In this process strong QCD (sQCD) is born as the theory describing the interaction of colored quarks and gluons. These are the phenomena that we are exploring at Jefferson Lab and other accelerators around the world - the full discovery of the baryon (and meson) spectrum, the role of chiral symmetry breaking and the generation of dynamical quark mass in confinement. While we cannot recreate in the laboratory the exact condition that occurred during this period in the universe, with existing accelerators we can explore these processes in relative isolation. With electron machines and high energy photon beams in

the few GeV energy range we search for undiscovered nucleon and baryon excitations.

As the universe expands and cools down the coupling of quarks to the gluon field becomes stronger and quarks become more massive and form excited states in abundance. This eventually leads to the forming of stable nucleons.

## 2 The quest for the missing baryon states

The excited states of the nucleon have been studied experimentally since the 1950's [4]. They contributed to the discovery of the quark model in 1964 by Gell-Mann [5] and Zweig [6], and were critical for the discovery of "color" degrees of freedom as introduced by Greenberg [7]. The quark structure of baryons resulted in the prediction of a wealth of excited states with underlying spin-flavor and orbital symmetry of  $SU(6) \otimes O(3)$ , and led to a broad experimental effort to search for these states. Most of the initially observed states were found with hadronic probes. However, of the many excited states predicted in the quark model, only a fraction have been observed to date.

It is interesting to point out recent findings that relate the observed baryon spectrum of different quark flavors with the baryon densities in the freeze out temperature in heavy ion collisions, which show evidence for missing baryons in the strangeness and the charm baryon sector [8,9]. These data hint that an improved baryon model including further unobserved light quark baryons would resolve the current discrepancy between hot QCD lattice results and the results obtained using a baryon resonance model that includes only states listed by the PDG. A complete accounting of excited baryon states of all flavors seems essential for a quantitative description of the occurrence of baryons in the evolution of the microsecond old universe. It makes a systematic search for so far undiscovered nucleon states even more compelling.

Search for the "missing" states and detailed studies of the resonance structure are now mostly carried out using electromagnetic probes and have been a major focus of hadron physics for the past two decades [10]. A broad experimental effort has been underway with measurements of exclusive meson photoproduction and electroproduction reactions, including many polarization observables. Precision data and the development of multi-channel partial wave analysis procedures have resulted in the discovery of several new excited states of the nucleon, which have been entered in the Review of Particle Physics (RPP) [11], and additional ones may be entered in subsequent editions.

The importance and impact of nucleon spectroscopy for sQCD may be compared with the impact that atomic spectroscopy had on the development of QED. It is through a complete description of the entire atomic spectroscopy and small effects, such as the Lamb shift, that QED is considered as fully established. In analogy, sQCD must be able to predict the nucleon spectrum, its pole structure and exact energy dependences before we can claim that the problem has been solved and we understand the spectrum. Of course, this in turn requires that the nucleon spectrum is experimentally fully established, a

charge to us experimentalists to do our part. It requires a "global" approach, employing different experimental equipments and beams, and a systematic search for undiscovered baryon states. A quantitative description of baryon spectroscopy and the structure of excited nucleons must eventually involve solving QCD for a complex strongly interacting multi-particle system. Recent advances in Lattice QCD led to predictions of the nucleon spectrum in QCD with dynamical quarks [12], albeit with still large pion masses of 396 MeV. At the present time predictions can therefore only be taken as indicative of the quantum numbers of excited states and not of the energy levels and pole structure of specific states. In parallel, the development of dynamical coupled channel models is being pursued with new vigor. The EBAC group at JLab has confirmed [13] that dynamical effects can result in significant mass shifts of the excited states. As a particularly striking result, a very large shift was found for the Roper resonance pole mass to  $\approx 1360$  MeV downward from its bare core mass of 1736 MeV. This result has clarified the longstanding puzzle of the incorrect mass ordering of  $N(1440)1/2^+$  and  $N(1535)1/2^-$  resonances in the constituent quark model. Developments on the phenomenological side go hand in hand with a world-wide experimental effort to produce high precision data in many different channel as a basis for a determination of the light-quark baryon resonance spectrum. On the example of experimental results from CLAS, the strong impact of precise meson photoproduction data is discussed. Several reviews have recently been published on the baryon spectrum and structure of excited states [14, 15, 16, 17, 18, 19], and on the 50 years puzzle of the Roper resonance [20].

Accounting for the complete excitation spectrum of the nucleon (protons and neutrons) and understanding the effective degrees of freedom is among the most important and certainly the most challenging task of hadron physics. The experimental  $N^*$  program currently focusses on the search for new excited states in the light-quark sector of  $N^*$  and  $\Delta^*$  states and in the mass range up to 2.5 GeV using energy-tagged photon beams in the few GeV range. Employing meson electroproduction the study of the internal structure of prominent resonances has been another major focus of the experimental exploration with CLAS.

### 3 Completing the $N^*$ and $\Delta^*$ Spectrum

The complex structure of the light-quark baryon spectrum complicates the experimental search for individual states. As a consequence of the strong interaction, resonances are wide, often 200 MeV to 350 MeV, and are difficult to be uniquely identified when only differential cross sections are measured. Most of the excited nucleon states listed in the Review of Particle Physics prior to 2010 have been observed in elastic pion scattering  $\pi N \rightarrow \pi N$ . However there are important limitations in the sensitivity to the higher mass nucleon states that may have small  $\Gamma_{\pi N}$  decay widths. The extraction of resonance contributions then becomes exceedingly difficult in  $\pi N$  scattering.

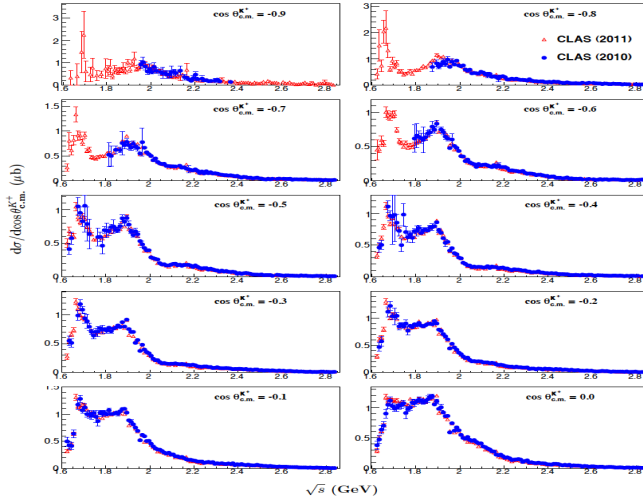


**Fig. 2** Invariant  $K\Lambda$  mass dependence of differential cross sections in bins of  $\cos\theta_{c.m.}^K$ .

Estimates for alternative decay channels have been made in quark model calculations [21] for various channels. This has led to a major experimental effort at JLab, ELSA, GRAAL, and MAMI, LEPS and other laboratories to chart differential cross sections and polarization observables for a variety of meson photoproduction channels. At JLab with CLAS, many final states have been measured with high precision [22, 23, 24, 25, 26, 27, 28, 29, 30, 31, 32, 33, 34] and are now employed in multi-channel analyses.

### 3.1 New excited nucleon states from open strangeness photoproduction

In the past decade one focus has been on measurements of  $\gamma p \rightarrow K^+ \Lambda$ , using a polarized photon beam several polarization observables can be measured by analyzing the parity violating decay of the recoil  $\Lambda \rightarrow p\pi^-$ . It is well known that the energy-dependence of a partial-wave amplitude for one particular channel is influenced by other reaction channels due to unitarity constraints. To fully describe the energy-dependence of an amplitude one has to include other reaction channels in a coupled-channel approach. Such analyses have been developed by the Bonn-Gatchina group [36], at JLab [37], Bonn-Jülich [38], Argonne-Osaka [39], and other groups.

The data sets with the highest impact on resonance amplitudes in the mass range above 1.7 GeV have been kaon-hyperon production using a spin-polarized photon beam and where the polarization of the  $\Lambda$  or  $\Sigma^0$  is also measured. The high precision cross section and polarization data [27, 28, 29, 30, 31] provide nearly full polar angle coverage and span the  $K^+ \Lambda$  invariant mass

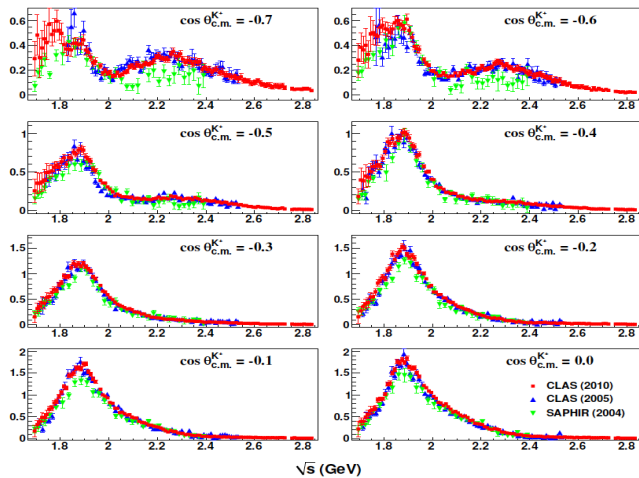


**Fig. 3** Invariant mass dependence of the  $\gamma p \rightarrow K^+ \Sigma^0$  differential cross section in the backward polar angle range.

range from threshold to 2.9 GeV, hence covering the full nucleon resonance domain where new states might be discovered.

The backward angles  $K^+ \Lambda$  data in Fig.2 show clear resonance-like structures at 1.7 GeV and 1.9 GeV that are particularly prominent and well-separated from other structures, while at more forward angles (not shown) t-channel processes become prominent and dominate the cross section. The broad enhancement at 2.2 GeV may also indicate resonant behavior although it is less visible at more central angles with larger background contributions. The  $K^+ \Sigma$  channel also indicates significant resonant behavior as seen in Fig. 3. The peak structure at 1.9 GeV is present at all angles with a maximum strength near 90 degrees, consistent with the behavior of a  $J^P = 3/2^+$  p-wave. Other structures near 2.2 to 2.3 GeV are also visible. Still, only a full partial wave analysis can determine the underlying resonances, their masses and spin-parity. The task is somewhat easier for the  $K\Lambda$  channel, as the iso-scalar nature of the  $\Lambda$  selects isospin- $\frac{1}{2}$  states to contribute to the  $K\Lambda$  final state, while both isospin- $\frac{1}{2}$  and isospin- $\frac{3}{2}$  states can contribute to the  $K\Sigma$  final state.

These cross section data together with the  $\Lambda$  and  $\Sigma$  recoil polarization and polarization transfer data to the  $\Lambda$  and  $\Sigma$  had strong impact on the discovery of several new nucleon states. They also provided new evidence for several candidate states that had been observed previously but lacked confirmation, as shown in Fig. 4. It is interesting to observe that five of the observed nucleon states have nearly degenerate masses near 1.9 GeV. Similarly, the new  $\Delta$  state appears to complete a mass degenerate multiplet near 1.9 GeV as well. There is no obvious mechanism for this apparent degeneracy. Nonetheless, all new states

may be accommodated within the symmetric constituent quark model based on  $SU(6) \otimes O(3)$  symmetry group as far as quantum numbers are concerned. As discussed in section 1 for the case of the Roper resonance  $N(1440)\frac{1}{2}^+$ , the masses of all pure quark model states need to be corrected for dynamical coupled channel effects to compare them with observed resonances. The same applies to the recent Lattice QCD predictions [40] for the  $N^*$  and  $\Delta^*$  spectra.

### 3.2 A new high-mass isospin 3/2 state confirmed in the $N\pi$ final state

The power of polarization measurements has been demonstrated in the strong evidence seen for the  $\Delta(2200)7/2^-$  state. Although the state couples to  $N\pi$  with a branching ratio of just 3.5%, the combination of precise differential cross section and single and double polarization measurements made this possible [41]. Figure 5 shows the mass scan for the well known  $\Delta(1950)7/2^+$  and the new  $\Delta(2200)7/2^-$  showing clear effects on the effective  $\Delta\chi^2$ . The state had prior only a one-star rating. Its empirical mass value is indicated in Fig. 4 with the open green frame.

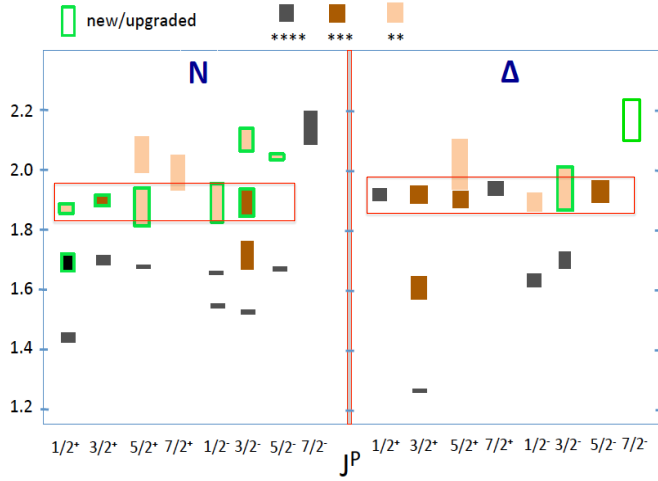


**Fig. 4** Nucleon and  $\Delta$  resonance spectrum up to 2.2 GeV in RPP 2016 [11]. The new states and states with improved evidence observed in the recent Bonn-Gatchina multi-channel analysis are shown with the green frame. The red frames highlight the apparent mass degeneracy of five or six states with different spin and parity. The analysis includes all the  $K^+\Lambda$  and  $K^+\Sigma^0$  cross section and polarization data.

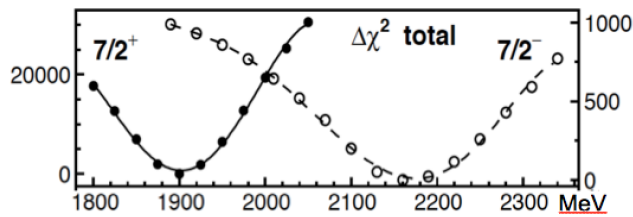


**Fig. 5** Evidence for  $\Delta(2200)7/2^-$  from  $\gamma p \rightarrow N\pi$  differential cross sections and single and double polarization measurements at CLAS and CBELSA. Evidence has also been observed in  $K\Sigma$  and  $p\pi^0\eta$  final states.

### 3.3 Vector meson photoproduction

In the mass range above 2.0 GeV resonances tend to decouple from simple 2-body final states like  $N\pi$ ,  $N\eta$ , and  $K\Lambda$ . We have to consider more complex final states with multi-mesons, such as  $N\pi\pi$  and  $N\pi\eta$ , as well as vector mesons  $N\omega$ ,  $N\phi$ , and  $K^*\Sigma$ . The study of such final states adds significant complexity as more amplitudes can contribute to photoproduction of spin-1 mesons, compared to pseudo-scalar meson production. As is the case for  $N\eta$  production, the  $N\omega$  channel is selective to isospin  $\frac{1}{2}$  nucleon states. CLAS has collected a tremendous amount of data in the  $p\omega$  [25,26,44],  $p\phi$  [42,43], and  $K^*\Sigma$  [35] final states on differential cross sections and spin-density matrix elements, that are now entering into the more complex multi-channel analyses such as Bonn-Gatchina. The CLAS collaboration performed a single channel event-based analysis, and provide further evidence for the  $N(2000)5/2^+$ .

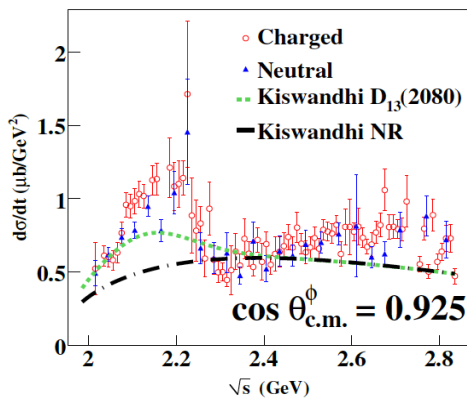


**Fig. 6** Differential cross sections of  $\gamma p \rightarrow p\phi$  production for the most forward angle bin. The two curves refer to fits without (dashed) and with (dotted) a known resonance at 2.08 GeV included.



Photoproduction of  $\phi$  mesons is also considered a potentially rich source of new excited nucleon states in the mass range above 2 GeV. Some lower mass states such as  $N(1535)1/2^-$  below the  $N\phi$  threshold may have significant  $s\bar{s}$  components [45]. Such components may result in states coupling to  $p\phi$  with significant strength above threshold. Differential cross sections and spin-density matrix elements have been measured for  $\gamma p \rightarrow p\phi$  in a mass range up to nearly 3 GeV. A multi-channel partial wave analysis is required to pull out any significant resonance strength in this channel. Figure 6 shows the differential cross section  $d\sigma/dt$  of the most forward angle bin. A broad structure at 2.2 GeV is present, but does not show the typical Breit-Wigner behavior of a single resonance. It also does not fit the data in a larger angle range, which indicates that contributions other than genuine resonances may be significant. The forward and backward angle structures may also hint at the presence of dynamical effects possibly due to molecular contributions such as diquark-antitriquark contributions [46], the strangeness equivalent to the recently observed hidden charm  $P_c^+$  states.

Another process that has promise in the search for new excited baryon states, including those with isospin-3/2, is  $\gamma p \rightarrow K^*\Sigma$ . In distinction to the vector mesons discussed above, diffractive processes do not play a role in this channel, which then may allow more direct access to s-channel resonance production.

We can conclude that meson photoproduction has become an essential tool in the search for new excited baryons. The exploration of the internal structure of excited states and the effective degrees of freedom contributing to s-channel resonance excitation requires the use of electron beams, where the virtuality  $Q^2$  of the exchanged photon can be varied to probe the spatial structure (Fig. 7). This is discussed in the following section.

#### 4 Structure of excited nucleons

This will enable us to draw some conclusions about the effective degrees of freedom underlying the resonance transition strength. The fact that resonance can exhibit very different  $Q^2$ -dependencies in their respective helicity amplitudes is demonstrated with the 3 panels in Figure 8 where integrated cross sections are displayed taken at different photon virtuality  $Q^2$ . They exhibit a number of enhancements that are associated with several prominent resonance, the  $\Delta(1232)3/2^+$ , the Roper  $N(1440)1/2^+$ ,  $N(1520)3/2^-$ , and  $N(1680)5/2^+$ . The strength of the  $\Delta$  excitation seen at small  $Q^2$  drops rapidly at higher  $Q^2$ . The Roper  $N(1440)1/2^+$  is not visible at low  $Q^2$  but emerges as  $Q^2$  increases. The  $N(1520)3/2^-$  and  $N(1535)1/2^-$  bump is small at low  $Q^2$  and becomes the dominant peak at highest  $Q^2$ . This  $Q^2$  dependence shows that the various underlying resonances behave differently with the increase in  $Q^2$ , which is indicative of different degrees-of-freedom underlying their respective excitation strengths.

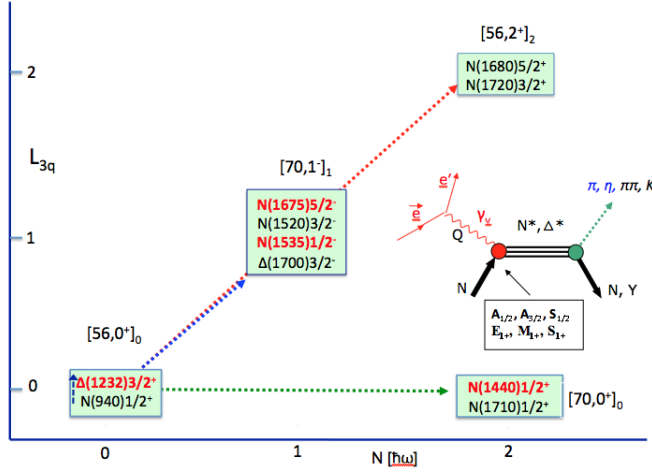


**Fig. 7** Schematic of  $SU(6) \otimes O(3)$  supermultiplets with selected prominent excited states that have been explored in  $ep \rightarrow e'\pi^+n$ ,  $ep \rightarrow e'p'\pi^0$  and  $ep \rightarrow e'p'\pi^+\pi^-$ . Only the states highlighted in red are discussed here. The insert shows the helicity amplitudes and electromagnetic multipoles extracted from the data.

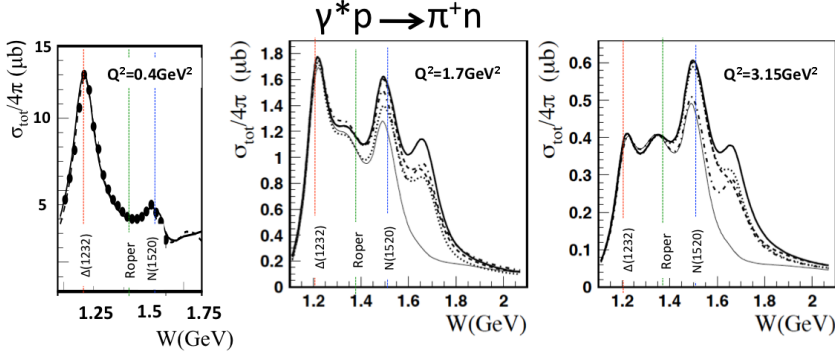


**Fig. 8** Evolution of the resonance strength with  $Q^2$ . The 3 panels show the strength of the 4 enhancements, which are related dominantly to certain resonances, vary with increasing  $Q^2$  significantly.

Electroproduction of final states with pseudoscalar mesons (e.g.  $N\pi$ ,  $p\eta$ ,  $K\Lambda$ ) have been employed with CLAS, leading to new insights into the dependence of effective degrees of freedom on the distance scale, e.g. meson-baryon, constituent quarks, dressed quarks, and bare quark contributions. Several excited states, shown in Fig. 7 assigned to their primary  $SU(6) \otimes O(3)$  supermultiplets, have been studied. The  $p\Delta^+(1232)3/2^+$  transition is now well measured in a large range of  $Q^2$  [47, 48, 49, 50]. The transition amplitudes, characterizing the  $N - \Delta(1232)$  transition, are usually defined as the magnetic transition form factor  $G_M^\Delta$ , the electric quadrupole ratio  $R_{EM} = E_{1+}/M_{1+}$  and the scalar quadrupole ratio  $R_{SM} = S_{1+}/M_{1+}$ . The current status of these quantities are

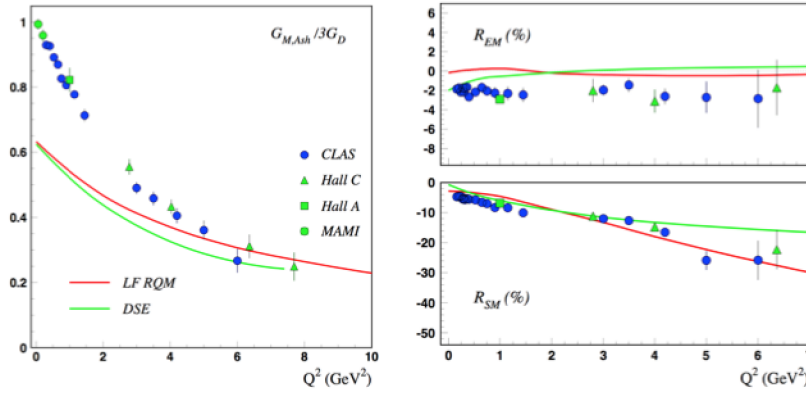


**Fig. 9** Left panel:  $N\Delta$  transition magnetic form factor. Right panel: Electric quadrupole ratio  $R_{EM}$  (top), and scalar quadrupole ratio  $R_{SM}$  (bottom).

shown in Fig. 9. The data are compared to two recent calculations, one based on the LF/RQM [59], and on the DSE/QCD approach [60]. For the magnetic transition form factor both calculations are close to each other, and agree with the data at the high  $Q^2$  end. Both calculations project very small  $R_{EM}$  quark contributions throughout the measured  $Q^2$  range. They show similar trends for  $R_{SM}$  at low and medium  $Q^2$ , but are diverging at the highest  $Q^2$ . Extending the data to even higher  $Q^2$  should be revealing. Asymptotic QCD predicts a constant value for  $R_{SM}$ , while holographic QCD models predict a specific limit of  $R_{SM}(Q^2 \rightarrow \infty) \rightarrow -1$  [61].

Two of the prominent higher mass states, the Roper resonance  $N(1440)1/2^+$  and  $N(1535)1/2^-$  are shown in Fig. 10 as representative examples [50, 51] from a wide program at JLab [52, 53, 54, 55, 56, 57]. For these two states advanced relativistic quark model calculations [58] and QCD-linked calculations from Dyson-Schwinger equations [62] as well as Light Cone sum rule (LCSR) [63] have become available, for the first time employing QCD-based modeling of the excitation of the quark core. There is near quantitative agreement of both calculations with the data at  $Q^2 > 1.5 \text{ GeV}^2$ . Note that the LF RQM includes a momentum-dependent quark mass parameterization that is fixed to describe the nucleon electromagnetic form factors. The same function is used for all transition amplitudes. This result strongly indicates that at the scale of the quark core the Roper resonance is the first radial excitation of the nucleon. From the excellent agreement with LF RQM and the LC SR approaches we can also draw the conclusions the the  $N(1535)1/2^-$  resonance as its core is the first orbital excitation of the nucleon. . We want to emphasize, however, it is only from the measurement of the excitation strength at high enough  $Q^2$  that we can draw such conclusions [20, 16], while the peripheral behavior at low  $Q^2$  requires the inclusion of hadronic degrees-of-freedom for a quantitative description. For the Roper resonance such contributions have been

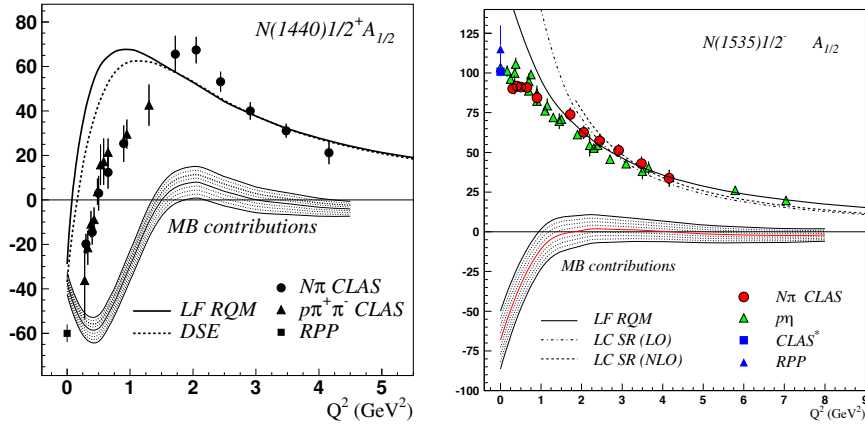


**Fig. 10** Left panel: The transverse helicity amplitudes  $A_{1/2}$  for the Roper resonance  $N(1440)1/2^+$ . Data are from CLAS compared to the LF RQM with momentum-dependent quark masses and with projections from the DSE approach. The dashed band indicates size of non 3-quark contributions obtained from a the difference of the LF RQM curve and the CLAS data. The right panel shows the  $A_{1/2}$  amplitude for the  $N(1535)1/2^-$  compared to LF RQM calculations and to lattice QCD-based Light Cone Sum Rule calculation in LO and NLO approximation [63].

described successfully in dynamical meson-baryon models [64] and in effective field theory [65].

Knowledge of the helicity amplitudes in a large  $Q^2$  range allows for the determination of the transition charge densities on the light cone in transverse impact parameter space  $(b_x, b_y)$  [66]. Figure 11 shows the comparison of  $N(1440)1/2^+$  and  $N(1535)1/2^-$ . There are clear differences in the charge transition densities between the two states. The Roper resonance has a softer positive core and a wider negative outer cloud than  $N(1535)$ . It also exhibits a larger shift in  $b_y$  when the transition is from a proton that is polarized along the  $b_x$  axis. Both transitions show an electric transition dipole moment, the one of the Roper appears as significantly stronger and shows a more pronounced charge asymmetry.

As these transition charge densities represent moments of transition amplitudes they may be accessible to LQCD and other implementations of sQCD.

#### 4.1 The $N(1675)5/2^-$ state - revealing the meson-baryon contributions

In previous discussions we have assumed that meson-baryon degrees of freedom provide significant strength to the resonance excitation in the low  $Q^2$  domain where quark based approaches LF RQM, DSE/QCD, and LCSR calculations fail to reproduce the transition amplitudes quantitatively. Our conclusion rests, in part, with this assumption. But, how can we be certain of the validity of this assumption?

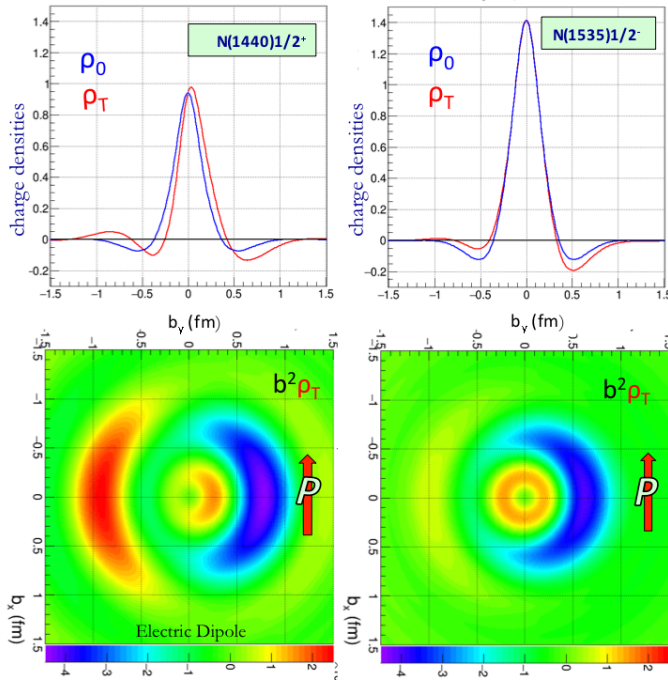


**Fig. 11** Charge densities for the two resonances. Left panels:  $N(1440)1/2^+$ , top: projection of transition charge densities on  $b_y$ , bottom: transition charge densities when the proton is spin polarized along  $b_x$ . Right panels: same for  $N(1535)1/2^-$ . Note that the densities are scaled with  $b^2$  to emphasize the outer wings. Color code: negative charge tends to blue, positive charge tends to red. For ease of comparison all scales are the same. Figures courtesy of F.X. Girod.

The  $N(1675)5/2^-$  resonance allows testing this assumption, quantitatively. Figure 12 shows our current knowledge of the transverse helicity amplitude  $A_{1/2}(Q^2)$  for the proton and the neutron and LF RQM [69] and hypercentral CQM [70] calculations. The specific quark transition for a  $J^P = 5/2^-$  state belonging to the  $SU(6) \otimes O(3) = [70, 1^-]$  supermultiplet configuration prohibits the transition from the proton in a single quark transition. This suppression is known as the Moorhouse selection rule [68], and is valid for the transverse transition amplitudes  $A_{1/2}$  and  $A_{3/2}$  at all  $Q^2$ . It should be noted that this selection rule does apply only to the transition from protons but not from neutrons. Modern quark models, that go beyond single quark transitions, confirm quantitatively the suppression resulting in very small transition amplitudes from protons but large ones from neutrons. The measured helicity amplitudes off the protons are almost exclusively due to meson-baryon contributions as the dynamical coupled channel (DCC) calculation indicates (dashed line). The quark model prediction on the neutron predict large amplitudes at the photon point consistent with the single data point. Note that the differences data-model for the proton and for the neutron have opposite signs but are of about

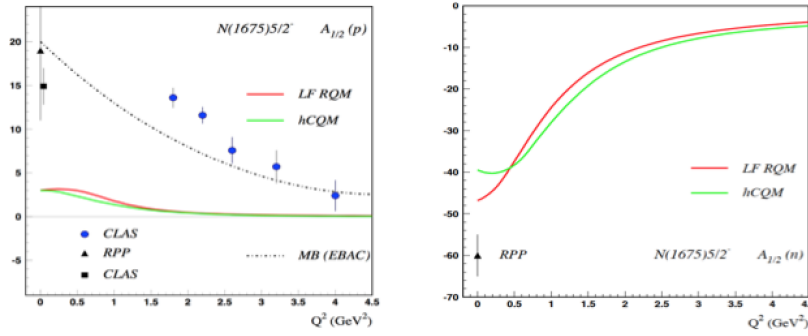


**Fig. 12** Helicity amplitude  $A_{1/2}$  for  $N^+(1675)5/2^-$  off proton target (left), and for  $N^0(1675)5/2^-$  off neutron target (right).

the same magnitude of  $\Delta A_{1/2}^p(0) = 16 \pm 8 \times 10^{-3} \text{GeV}^{-1}$ , and  $\Delta A_{1/2}^n(0) = -13 \pm 5 \times 10^{-3} \text{GeV}^{-1}$ . A very similar behavior is seen for the  $A_{3/2}$  amplitudes  $\Delta A_{3/2}^p(0) = 15 \pm 5 \times 10^{-3} \text{GeV}^{-1}$ , and  $\Delta A_{3/2}^n(0) = -23 \pm 10 \times 10^{-3} \text{GeV}^{-1}$  [69]. The close correlation of the DCC calculation and the measured data for the case when quark contributions are nearly absent, supports the phenomenological description of the helicity amplitudes in terms of a 3-quark core that dominate at high  $Q^2$  and meson-baryon contributions that can make important contributions at lower  $Q^2$ .

## 5 Conclusions and Outlook

Over the past several years, eight light-quark baryon states in the mass range from 1.85 to 2.25 GeV have been either discovered, or evidence for their existence has been brought close to certainty. To a large degree this is the result of adding very precise photoproduction data in open strangeness channels to the data base that is included in multi-channel partial wave analyses. The measurement of polarization observables in these processes has been critical. In the mass range above 2 GeV more complex processes such as vector mesons or  $\Delta\pi$  may have sensitivity to states with higher masses and require more complex analyses techniques. Precision data in such channels have been available for a few years, but they have not been fully incorporated in multi-channel partial wave analyses processes.

There has been progress to predict the nucleon spectrum from first principles within QCD on the lattice. While pion masses of about 400 MeV are still too large for precise predictions of resonance masses and poles, the predicted quantum numbers coincide with  $SU(6)$  symmetry and states predicted within constituent quark models.

The light-quark baryon spectrum is likely also populated with hybrid excitations [12], where the gluonic admixtures to the wave function are dominating the excitation. These states appear with the same quantum numbers as ordinary quark excitations, and can only be isolated from ordinary states due to the  $Q^2$  dependence of their helicity amplitudes [67], which is expected to be quite different from ordinary quark excitations. To search for these new hybrid states, new electroproduction data especially at low  $Q^2$  [72] are needed, with different final states and at masses above 2 GeV.

On the theoretical side, we have seen the first calculation of the resonance transition helicity amplitudes and transition form factors for the case of the  $\Delta(1232)3/2^+$ , the Roper  $N(1440)1/2^+$ , and the  $N(1535)1/2^-$  within QCD-linked approaches. Here we see agreement with data is in the range of  $Q^2 > 2 - 3 \text{ GeV}^2$ . We also have seen that newly discovered nucleon resonances fit into the spectrum projected from LQCD with their quantum, albeit not (yet) with their mass assignments.

Despite the very significant progress made in recent years to further establish the light-quark baryon spectrum and explore the internal structure of excited states, much remains to be done. A vast amount of precision data that have already been collected, must be included in the multi-channel analysis frameworks, and many polarization data sets are still to be analyzed. There are new data on 2-pion electroproduction [71] that will extend the mass range for the extraction of transition helicity amplitudes for high mass resonances. Of particular interest is here the  $N(1900)3/2^+$ , which only recently has become a well established excited nucleon state. There are also upcoming experiments to study resonance excitations at much higher  $Q^2$  and with higher statistical precision at Jefferson Lab with CLAS12 [73] that may begin to reveal the transition to the bare quark core contributions at short distances.

Let me finally conclude, that the community is still on track of fulfilling Nathan Isgur's vision of a 30 year program to solve the puzzle of the baryon spectrum.

**Acknowledgements** I want to thank Inna Aznauryan for providing the figures on the transition amplitudes, which have led to new insight into the degrees of freedom underlying resonance excitations. I also thank Ralf Gothe, Viktor Mokeev and Craig Roberts for numerous discussions on the subjects discussed in this presentation, and F.X. Girod for providing the color graphics in Fig. 11. This work was supported by the U.S. Department of Energy, Office of Science, Office of Nuclear Physics, under Contract No. DE-AC05-06OR23177.

## References

1. F. W. Dyson, A. S. Eddington and C. Davidson, Phil. Trans. Roy. Soc. Lond. A **220**, 291 (1920).
2. A. Einstein, Annalen Phys. **49**, no. 7, 769 (1916) [Annalen Phys. **14**, 517 (2005)].
3. S. Capstick and N. Isgur, Phys. Rev. D **34**, 2809 (1986)
4. H. L. Anderson, E. Fermi, E. A. Long and D. E. Nagle (1952) Phys. Rev. **85**, 936 .
5. M. Gell-Mann, "A Schematic Model of Baryons and Mesons," Phys. Lett. **8**, 214 (1964).
6. G. Zweig, "An SU(3) model for strong interaction symmetry and its breaking," CERN-TH-401 and 412 (1964)

7. O. W. Greenberg, Phys. Rev. Lett. **13**, 598 (1964)
8. A. Bazavov *et al.*, Phys. Rev. Lett. **113**, no. 7, 072001 (2014)
9. A. Bazavov *et al.*, Phys. Lett. B **737**, 210 (2014)
10. V. D. Burkert and T. S. H. Lee Int. J. Mod. Phys. E **13**, 1035 (2004).
11. C. Patrignani *et al.* [Particle Data Group], Chin. Phys. C **40**, no. 10, 100001 (2016).
12. J. J. Dudek and R. G. Edwards, Phys. Rev. D **85**, 054016 (2012)
13. N. Suzuki *et al.*, Phys. Rev. Lett. **104**, 042302 (2010)
14. E. Klempt and J. M. Richard, Rev. Mod. Phys. **82**, 1095 (2010)
15. L. Tiator, D. Drechsel, S. S. Kamalov and M. Vanderhaeghen, Eur. Phys. J. ST **198**, 141 (2011).
16. I. G. Aznauryan and V. D. Burkert, Prog. Part. Nucl. Phys. **67**, 1 (2012)
17. I. G. Aznauryan *et al.*, Int. J. Mod. Phys. E **22**, 1330015 (2013)
18. V. Crede and W. Roberts, Rept. Prog. Phys. **76**, 076301 (2013)
19. V. I. Mokeev *et al.*, Phys. Rev. C **93**, no. 2, 025206 (2016)
20. V. D. Burkert and C. D. Roberts, arXiv:1710.02549 [nucl-ex].
21. S. Capstick and W. Roberts, Phys. Rev. D **49**, 4570 (1994)
22. M. Dugger *et al.*, Phys. Rev. Lett. **96**, 062001 (2006) [Phys. Rev. Lett. **96**, 169905 (2006)]
23. M. Dugger *et al.* [CLAS Collaboration], Phys. Rev. C **79**, 065206 (2009)
24. M. Williams *et al.* [CLAS Collaboration], Phys. Rev. C **80**, 045213 (2009)
25. M. Williams *et al.* [CLAS Collaboration], Phys. Rev. C **80**, 065209 (2009)
26. M. Williams *et al.* [CLAS Collaboration], Phys. Rev. C **80**, 065208 (2009)
27. R. K. Bradford *et al.* [CLAS Collaboration], Phys. Rev. C **75**, 035205 (2007)
28. R. Bradford *et al.* [CLAS Collaboration], Phys. Rev. C **73**, 035202 (2006)
29. M. E. McCracken *et al.* [CLAS Collaboration], Phys. Rev. C **81**, 025201 (2010)
30. B. Dey *et al.* [CLAS Collaboration], Phys. Rev. C **82**, 025202 (2010)
31. J. W. C. McNabb *et al.* [CLAS Collaboration], Phys. Rev. C **69**, 042201 (2004)
32. C. A. Paterson *et al.* [CLAS Collaboration], Phys. Rev. C **93**, no. 6, 065201 (2016)
33. N. Compton *et al.* [CLAS Collaboration], Phys. Rev. C **96**, no. 6, 065201 (2017)
34. D. Ho *et al.* [CLAS Collaboration], Phys. Rev. Lett. **118** (2017) no.24, 242002
35. A. V. Anisovich *et al.* [CLAS Collaboration], Phys. Lett. B **771**, 142 (2017).
36. A. Anisovich, R. Beck, E. Klempt, V. Nikonov, A. Sarantsev and U. Thoma, Eur. Phys. J. A **48**, 15 (2012)
37. B. Julia-Diaz, T.-S. H. Lee, A. Matsuyama and T. Sato, Phys. Rev. C **76**, 065201 (2007)
38. D. Rönchen *et al.*, Eur. Phys. J. A **50**, no. 6, 101 (2014)
39. H. Kamano, S. X. Nakamura, T.-S. H. Lee and T. Sato, Phys. Rev. C **88**, no. 3, 035209 (2013)
40. R. G. Edwards, J. J. Dudek, D. G. Richards and S. J. Wallace, Phys. Rev. D **84**, 074508 (2011)
41. A. V. Anisovich *et al.*, Phys. Lett. B **766**, 357 (2017)
42. H. Seraydaryan *et al.* [CLAS Collaboration], Phys. Rev. C **89**, no. 5, 055206 (2014)
43. B. Dey *et al.* [CLAS Collaboration], Phys. Rev. C **89**, no. 5, 055208 (2014)
44. P. Collins *et al.*, Phys. Lett. B **773**, 112 (2017)
45. B. C. Liu and B. S. Zou, Phys. Rev. Lett. **96**, 042002 (2006)
46. R. F. Lebed, Phys. Rev. D **92**, no. 11, 114030 (2015)
47. K. Joo *et al.* [CLAS Collaboration], Phys. Rev. Lett. **88**, 122001 (2002)
48. M. Ungaro *et al.* [CLAS Collaboration], Phys. Rev. Lett. **97**, 112003 (2006)
49. V. V. Frolov *et al.*, Phys. Rev. Lett. **82**, 45 (1999)
50. I. G. Aznauryan *et al.* [CLAS Collaboration], Phys. Rev. C **80**, 055203 (2009)
51. I. G. Aznauryan *et al.* [CLAS Collaboration], Phys. Rev. C **78**, 045209 (2008)
52. V. I. Mokeev *et al.* [CLAS Collaboration], Phys. Rev. C **86**, 035203 (2012)
53. H. Denizli *et al.* [CLAS Collaboration], Phys. Rev. C **76**, 015204 (2007)
54. C. S. Armstrong *et al.* [Jefferson Lab E94014 Collaboration], Phys. Rev. D **60**, 052004 (1999)
55. H. Egiyan *et al.* [CLAS Collaboration], Phys. Rev. C **73**, 025204 (2006)
56. K. Park *et al.* [CLAS Collaboration], Phys. Rev. C **77**, 015208 (2008)
57. K. Park *et al.* [CLAS Collaboration], Phys. Rev. C **91**, 045203 (2015)



58. I. G. Aznauryan and V. D. Burkert, Phys. Rev. C **92**, no. 3, 035211 (2015)
59. I. G. Aznauryan and V. D. Burkert, arXiv:1603.06692 [hep-ph].
60. J. Segovia, I. C. Cloet, C. D. Roberts and S. M. Schmidt, Few Body Syst. **55**, 1185 (2014)
61. H. R. Grigoryan, T.-S. H. Lee and H. U. Yee, Phys. Rev. D **80**, 055006 (2009)
62. J. Segovia et al., Phys. Rev. Lett. **115**, no. 17, 171801 (2015)
63. I. V. Anikin, V. M. Braun and N. Offen, Phys. Rev. D **92**, no. 1, 014018 (2015)
64. I. T. Obukhovskiy et al., Phys. Rev. D **84**, 014004 (2011)
65. T. Bauer, S. Scherer and L. Tiator, Phys. Rev. C **90**, no. 1, 015201 (2014)
66. L. Tiator and M. Vanderhaeghen, Phys. Lett. B **672**, 344 (2009)
67. Z. p. Li, V. Burkert and Z. j. Li, Phys. Rev. D **46**, 70 (1992).
68. R. G. Moorhouse, Phys. Rev. Lett. **16**, 772 (1966).
69. I. G. Aznauryan and V. Burkert, Phys. Rev. C **95**, no. 6, 065207 (2017)
70. E. Santopinto and M. M. Giannini, Phys. Rev. C **86**, 065202 (2012)
71. E. L. Isupov *et al.* [CLAS Collaboration], Phys. Rev. C **96**, no. 2, 025209 (2017)
72. A. D' Angelo et al., Jefferson Lab experiment E12-16-010 (2016).
73. R. Gothe et al., Jefferson Lab experiment E12-09-003 (2009).